



A machining accuracy improvement approach for a horizontal machining center based on analysis of geometric error characteristics

Peng Niu^{1,2} · Qiang Cheng^{1,2} · Zhifeng Liu^{1,2} · Hongyan Chu^{1,3}

Received: 18 July 2020 / Accepted: 21 December 2020 / Published online: 8 January 2021
© The Author(s), under exclusive licence to Springer-Verlag London Ltd. part of Springer Nature 2021

Abstract

In the actual production, it is expected to find several sensitivity geometric errors which have great influence on machining accuracy, so as to provide references for the manufacturing, assembly, and other links of the machine tool, and fundamentally improve the working performance. To study this problem, a novel global sensitivity analysis (GSA) method is proposed. Based on the MBS theory, the spatial error model is established to analyze the local influence of geometric error on machining accuracy. An improved second-order partial correlation coefficient based on the Pearson product moment is proposed to analyze the correlation between geometric errors. In addition, the error parameters will change greatly in the stroke of the moving parts. However, the rapid fluctuation of geometric error value will have a dynamic impact on the machining accuracy of machine tools, which is rarely noticed in the previous sensitivity analysis. This change is defined as the fluctuation of error. The high fitting degree function of error-displacement is obtained by using the high order Fourier series and sine series. Then, the fluctuation of the error in the machining stroke is analyzed by using the derivative of the function to the displacement. Through geometric error characteristics (including the local influence, correlation, and fluctuation) are studied comprehensively, the GSA of error is carried out. Finally, taking a machining center as an example and combining the sensitivity analysis results, the improvement measures are proposed to verify the correctness of the method.

Keywords Horizontal machining center (HMC) · Multi-body system (MBS) · Single geometric error fitting · Fourier series · Correlation coefficient · Global sensitivity analysis (GSA)

1 Introduction

The performance of HMC is mainly reflected in whether the quality of the products meets the accuracy requirements of users [1]. Machining accuracy is the main parameter and final goal of evaluating the working performance of machine tool [2]. Affected by many factors, such as the axial elongation [3] or “hot rise” of the spindle caused by heat during the long-term use of the spindle of HMC, which will directly affect the

accuracy of machine tool [4]. In addition, the installation and wear of the tool [5], the compression and deformation of the guide rail, the manufacturing error of the parts, and the complex human factors will reduce the machining accuracy of CNC machine tool. Among many factors, geometric error and thermal error account for about 50–70% of the total error, especially geometric error accounts for about 40% [6]. Machine tool geometric error has various types according to different forms, mainly including positioning error, straightness error, rolling error, Britain swing error, yaw error, and perpendicularity and parallelism error between motion axes. These errors interact with each other to influence the machine tool [7]. How to find and control effectively the key geometric errors which have great impact on machine tool is the main problem to improve machining accuracy.

To solve this problem, a novel global sensitivity analysis (GSA) is proposed. Sensitivity analysis (SA) can be used to study the influence of input uncertainty on system output [8], and also to identify the impact of system response by uncertainty changes from system parameters [9]. SA includes local

✉ Qiang Cheng
chengqiangbjut@126.com

¹ Institute of Advanced Manufacturing and Intelligent Technology, Beijing University of Technology, Beijing 100124, China

² Beijing Key Laboratory of Advanced Manufacturing Technology, Beijing University of Technology, Beijing 100124, China

³ Machinery Industry Key Laboratory of Heavy Machine Tool Digital Design and Testing Technology, Beijing University of Technology, Beijing 100124, China

sensitivity analysis (LSA) and GSA [10]. For CNC machine tools, LSA mainly analyzes the impact of a single error change on machining accuracy [11]. GSA considers the complex coupling effect of several geometric errors. Because the CNC machine tool is affected by many factors, the geometric errors have randomness, uncertainty, and mutual coupling and interaction [12]. Therefore, it is reasonable and effective to use GSA to identify critical geometric errors.

Many scholars have done a lot of research on GSA. Considering the randomness of geometric errors, Cheng et al. proposed the Sobol method to get the critical errors of a three-axis vertical machining center [13]. Xia used the improved Sobol method to identify globally the critical errors for a five-axis gear forming grinder [14]. Based on the Extended Fourier amplitude sensitivity test method, Guo et al. established the global sensitivity quantitative analysis method of geometric error for three-axis machining center [15]. Through the screw theory, Wu established the volume error model for three-axis machine tool, and studied the sensitivity of geometric error with this model [16]. However, in many sensitivity methods, it is neglected that the geometric error value changes with the displacement of motion axes. At different positions, the fluctuation of geometric errors should be considered. Therefore, a novel GSA method is proposed based on MBS and geometric error characteristics analysis.

Error modeling technology can clearly express the nonlinear mapping relationship between geometric error and machining accuracy. At present, modeling technology is becoming more and more mature, and MBS and screw theory are widely used [27]. Through the screw theory, Moon et al. carried out geometric error modeling and error compensation for CNC machine tools [17]. By the screw theory, Yang proposed a method to identify and correct position-independent geometric errors for multi-axis machine tools [18]. Based on MBS theory, Guo used homogeneous transformation matrix to establish geometric error model [19]. Similarly, Guo carried out geometric error modeling for five-axis machine tool with MBS theory and homogeneous transformation matrix [20]. With the development of MBS theory, it has become the mainstream choice of geometric error modeling [13, 14, 21].

Before studying the fluctuation of geometric errors with displacement, the fitting relationship between them must be established. At present, most polynomials with position coordinates as variables are chosen as fitting functions between single geometric error and displacement [16, 22, 23]. However, it is necessary to solve the order problem of the prediction model which has great influence on the fitting quality. Otherwise, the preset error will be introduced. Fu et al. [24] used automatic modeling technology to model single geometric error and selected the order of polynomials based on F-test. However, with the improvement of polynomial order, more measurement points were needed, and the fitting effect of polynomial form was not ideal compared with the actual error.

Compared with polynomial function fitting, composite function fitting with trigonometric function is better. According to the integral relationship between straightness error and angle error, Ekinci et al. used the composite function composed of sine and cosine function as the fitting function, which has a good fitting effect [25]. Tang et al. used the composite function composed of sine cosine function and parabola function to fit the surface curve of the guide rail scanned by the electron microscope, and then, the geometric error is predicted, which also revealed the internal relationship between the geometric error and the trigonometric function [26].

In this paper, Fourier series including constant term and sine cosine function is used to fit the relationship between single geometric error and displacement in a certain stroke of moving axis of machine tool. In the machining stroke (i.e., the stroke of the moving parts of the machine tool), the geometric error parameters vary greatly at different displacement points. This paper defines it as the fluctuation of error. The rapid fluctuation of geometric errors will inevitably have a dynamic impact on the machining accuracy of machine tools. After obtaining the function formula with a high fitting degree, the derivative of function to displacement is used to analyze the fluctuation of error. The derivative function is defined as the fluctuation function of geometric error. After the coordinates of each position point are substituted into the derivative function, the variation trend of the error at that point is obtained. Finally, the overall fluctuation of geometric error in the stroke will be obtained by averaging.

The correlation of geometric errors is objective [27, 28]. Cheng et al. introduced the Pearson correlation coefficient to analyze the correlation between geometric errors, and classified them by SPSS [29]. Chen et al. introduced the spearman rank correlation to study the relation between single error parameter and tool attitude error in the whole sampling space, and calculated and selected ten key error parameters with large absolute correlation coefficient [30]. In this paper, an improved second-order partial correlation coefficient based on the Pearson product moment is introduced to analyze the correlation between geometric errors. Partial correlation coefficient has been successfully applied to systems biology [31], genomics [32], and acoustics [33].

The general structure of this paper. Section 2 introduces the framework of the novel global sensitivity analysis method. In Section 3, an overview of the sensitivity analysis method is introduced. In Section 4, a case study is carried out to elaborate the methods used. Section 5 is the conclusion.

2 The framework of analysis method

In this paper, the machine tool geometric error model is established based on MBS theory, and the partial derivative

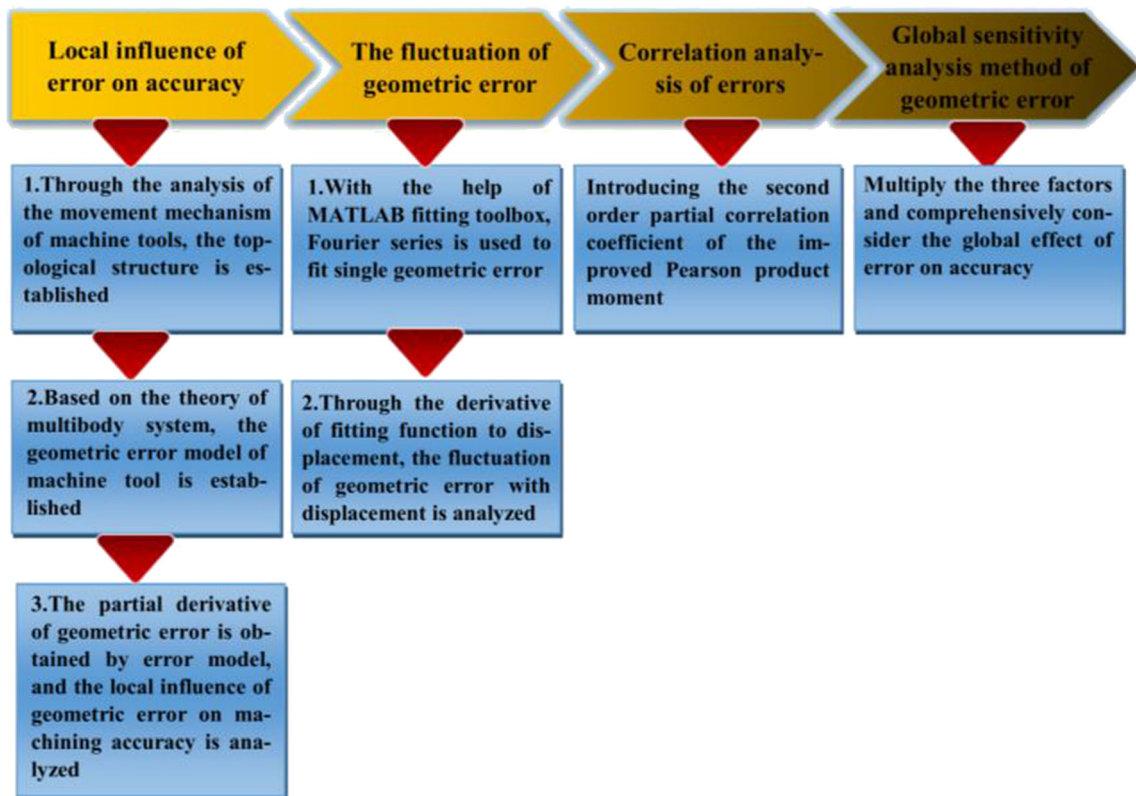
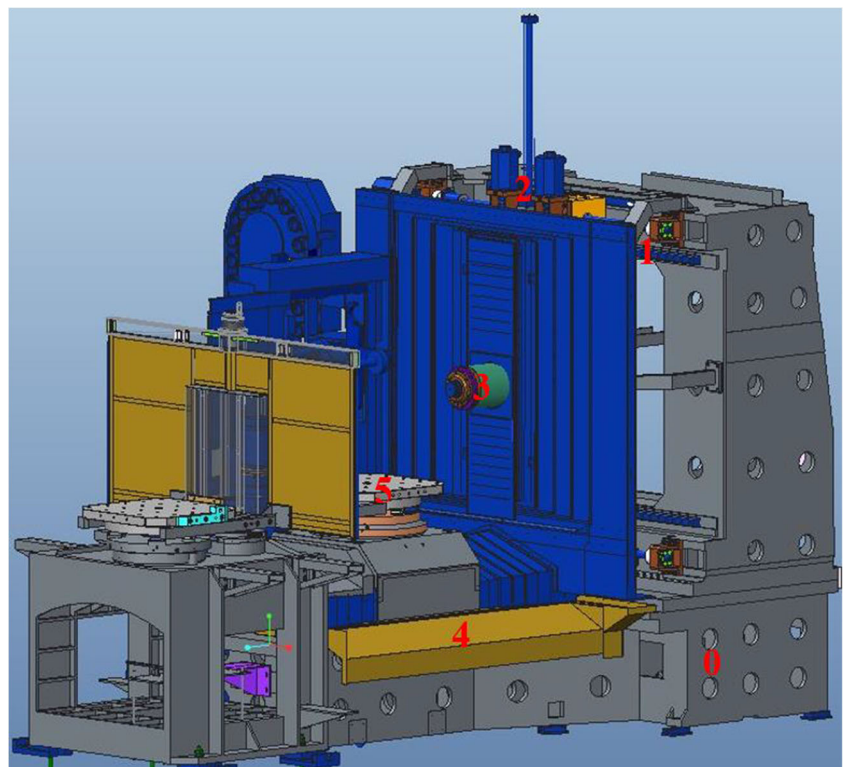


Fig. 1 Framework of global sensitivity analysis

of each geometric error is obtained. At the same time, considering the fluctuation and correlation of errors in the motion

stroke, the global sensitivity analysis model is constructed. The key geometric errors affecting the machining accuracy

Fig. 2 Structure of machine tool



are identified by the sensitivity coefficient. The framework of the global sensitivity analysis method involved in this paper is shown in Fig. 1.

3 Overview of sensitivity analysis method

3.1 Establishment of geometric error model

The machine tool structure is shown in Fig. 2. The mechanism of motion for the machine tool is analyzed, and the topological structure is established to represent the relative motion between moving axes. According to the motion transfer mode of the machine tool, the topological structure can be divided into two chains, as shown in Fig. 3. Set the fixed bed and column as inertia body with the mark of 0. X, Y, and Z guide rails are labeled 1, 2, and 4 respectively. The electric spindle

Table 1 Structural parameters of the machine tool

Main parameters (mm)	X-axis	1200
	Y-axis	950
	Z-axis	1100
Working table (mm)	width × length	630 × 630

and worktable are marked as 3 and 5 respectively. Table 1 shows the structural parameters of the machine tool.

This paper only studies the fluctuation of the errors with the displacement in the stroke of the motion axis. Therefore, during the error measurement, keep the workbench fixed and motionless with the workpiece, that is, the B-axis is still and there is no error. Table 2 shows the symbols and meanings of geometric errors. Based on MBS theory, the motion characteristic matrix of the CNC machine tool is established by using homogeneous coordinate transformation, as shown in Table 3.

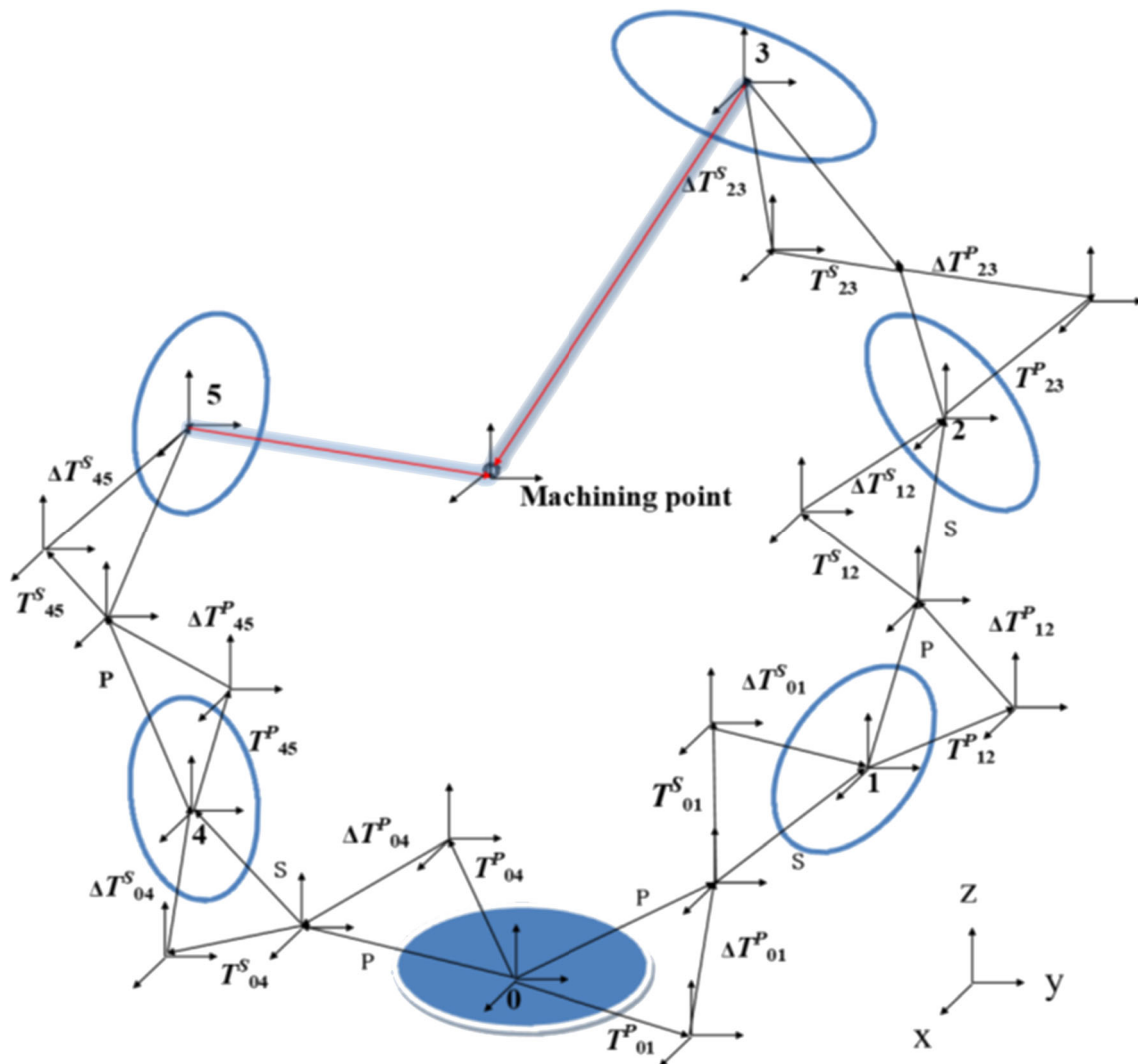


Fig. 3 Topological structure of machine tool

Table 2 Geometric error of HMC

Axis	Symbols	Meanings
X-axis	δx_x	Positioning error
	δy_x	Y direction of straightness error
	δz_x	Z direction of straightness error
	$\varepsilon \alpha_x$	Rolling error
	$\varepsilon \beta_x$	Britain swing error
	$\varepsilon \gamma_x$	Yaw error
Y-axis	δx_y	X direction of straightness error
	δy_y	Positioning error
	δz_y	Z direction of straightness error
	$\varepsilon \alpha_y$	Rolling error
	$\varepsilon \beta_y$	Britain swing error
	$\varepsilon \gamma_y$	Yaw error
Z-axis	δx_z	X direction of straightness error
	δy_z	Y direction of straightness error
	δz_z	Positioning error
	$\varepsilon \alpha_z$	Rolling error
	$\varepsilon \beta_z$	Britain swing error
	$\varepsilon \gamma_z$	Yaw error
Orientation errors	$\varepsilon \gamma_{xy}$	X, Y-axes perpendicularity error
	$\varepsilon \beta_{xz}$	X, Z-axes perpendicularity error
	$\varepsilon \alpha_{yz}$	Z, Y-axes perpendicularity error

In the table:
 The superscript p is static; The subscript s is motion;
 T is the error characteristic matrix in an ideal state;
 ΔT represents the error characteristic matrix in the actual state;

$I_{4 \times 4}$ denotes that when the error is relatively small, it can be ignored as the unit matrix;

Set the coordinates of the tool forming point in the tool coordinate system as:

$$P_t = [P_{tx} P_{ty} P_{tz} 1]^T \tag{1}$$

Set the coordinates of the workpiece forming point in the workpiece coordinate system as:

$$P_w = [P_{wx} P_{wy} P_{wz} 1]^T \tag{2}$$

When the machine tool works in the ideal state without error, the ideal coordinates of the workpiece forming point in the tool coordinate system can be written as:

$$P_{ideal} = [T_{01}^p T_{01}^s T_{12}^p T_{12}^s T_{23}^p T_{23}^s]^{-1} T_{04}^p T_{04}^s P_w \tag{3}$$

Table 3 The motion characteristic matrix of machine tool

Axis	Body ideal static, homogeneous transformation matrix of motion	Body static, homogeneous transformation matrix of kinematic error
X-axis	$T_{01}^p = I_{4 \times 4}$ $T_{01}^s = \begin{bmatrix} 1 & 0 & 0 & x \\ 0 & 1 & 0 & 0 \\ 0 & 0 & 1 & 0 \\ 0 & 0 & 0 & 1 \end{bmatrix}$	$\Delta T_{01}^p = I_{4 \times 4}$ $\Delta T_{01}^s = \begin{bmatrix} 1 & -\varepsilon \gamma_x & \varepsilon \beta_x & \delta x_x \\ \varepsilon \gamma_x & 1 & -\varepsilon \alpha_x & \delta y_x \\ -\varepsilon \beta_x & \varepsilon \alpha_x & 1 & \delta z_x \\ 0 & 0 & 0 & 1 \end{bmatrix}$
Y-axis	$T_{12}^p = I_{4 \times 4}$ $T_{12}^s = \begin{bmatrix} 1 & 0 & 0 & 0 \\ 0 & 1 & 0 & y \\ 0 & 0 & 1 & 0 \\ 0 & 0 & 0 & 1 \end{bmatrix}$	$\Delta T_{12}^p = \begin{bmatrix} 1 & -\varepsilon \gamma_{xy} & 0 & 0 \\ \varepsilon \gamma_{xy} & 1 & 0 & 0 \\ 0 & 0 & 1 & 0 \\ 0 & 0 & 0 & 1 \end{bmatrix}$ $\Delta T_{12}^s = \begin{bmatrix} 1 & -\varepsilon \gamma_y & \varepsilon \beta_y & \delta x_y \\ \varepsilon \gamma_y & 1 & -\varepsilon \alpha_y & \delta y_y \\ -\varepsilon \beta_y & \varepsilon \alpha_y & 1 & \delta z_y \\ 0 & 0 & 0 & 1 \end{bmatrix}$
Z-axis	$T_{04}^p = I_{4 \times 4}$ $T_{04}^s = \begin{bmatrix} 1 & 0 & 0 & 0 \\ 0 & 1 & 0 & 0 \\ 0 & 0 & 1 & z \\ 0 & 0 & 0 & 1 \end{bmatrix}$	$\Delta T_{04}^p = \begin{bmatrix} 1 & 0 & \varepsilon \beta_{xz} & 0 \\ 0 & 1 & -\varepsilon \alpha_{yz} & 0 \\ -\varepsilon \beta_{xz} & \varepsilon \alpha_{yz} & 1 & 0 \\ 0 & 0 & 0 & 1 \end{bmatrix}$ $\Delta T_{04}^s = \begin{bmatrix} 1 & -\varepsilon \gamma_z & \varepsilon \beta_z & \delta x_z \\ \varepsilon \gamma_z & 1 & -\varepsilon \alpha_z & \delta y_z \\ -\varepsilon \beta_z & \varepsilon \alpha_z & 1 & \delta z_z \\ 0 & 0 & 0 & 1 \end{bmatrix}$
B-axis	$T_{45}^p = I_{4 \times 4}$ $T_{45}^s = I_{4 \times 4}$	$\Delta T_{45}^p = I_{4 \times 4}$ $\Delta T_{45}^s = I_{4 \times 4}$

In the case of actual machining, the actual coordinates of the workpiece forming point in the tool coordinate system are:

$$P_{actual} = [\Delta T_{03}]^{-1} \Delta T_{04} P_w \tag{4}$$

Here,

$$\Delta T_{03} = T_{01}^p \Delta T_{01}^p T_{01}^s \Delta T_{01}^s T_{12}^p \Delta T_{12}^p T_{12}^s \Delta T_{12}^s T_{23}^p \Delta T_{23}^p T_{23}^s \Delta T_{23}^s ;$$

$$\Delta T_{04} = T_{04}^p \Delta T_{04}^p T_{04}^s \Delta T_{04}^s .$$

The comprehensive error matrix can be written by symbol $E(G)$ as follows:

$$E(G) = P_{ideal} - P_{actual} = \begin{bmatrix} E_x(G) \\ E_y(G) \\ E_z(G) \\ 0 \end{bmatrix} \tag{5}$$

The machining process of this paper is to analyze the machining accuracy when simulating the machining of fixed size workpiece under the fixed workpiece and cutter installation position. Therefore, P_w and x, y, z in Table 3 are predetermined values. $E_x(G), E_y(G), E_z(G)$ represent the machining accuracy function with geometric error as variable in three directions.

$G = [g_1, g_2, g_3, g_4, g_5, g_6, g_7, g_8, g_9, g_{10}, g_{11}, g_{12}, g_{13}, g_{14}, g_{15}, g_{16}, g_{17}, g_{18}]$ represents a vector composed of 18 errors, making $\delta x_x, \delta y_x, \delta z_x, \varepsilon \alpha_x, \varepsilon \beta_x, \varepsilon \gamma_x, \delta x_y, \delta y_y, \delta z_y, \varepsilon \alpha_y, \varepsilon \beta_y, \varepsilon \gamma_y, \delta x_z, \delta y_z, \delta z_z, \varepsilon \alpha_z, \varepsilon \beta_z, \varepsilon \gamma_z = g_1, g_2, g_3, g_4, g_5, g_6, g_7, g_8, g_9, g_{10}, g_{11}, g_{12}, g_{13}, g_{14}, g_{15}, g_{16}, g_{17}, g_{18}$.

3.2 Local influence analysis of geometric error

To analyze the local influence of single geometric error on machining accuracy of the machine tool, according to the formula (5), the partial derivative of the error is calculated by using the machining accuracy function according to formula (5). Taking the error $\delta x_x (=g_1)$ as an example, after the partial derivative of g_1 is calculated, the average value of the error measurement data is brought in, and the local influence on the machining accuracy in three directions when it changes slightly is analyzed. The matrix form represented by the symbol $f_{g_1}^{(1)}$ is:

$$f_{g_1}^{(1)} = \begin{bmatrix} \frac{\partial E_x}{\partial g_1} & 0 & 0 \\ 0 & \frac{\partial E_y}{\partial g_1} & 0 \\ 0 & 0 & \frac{\partial E_z}{\partial g_1} \end{bmatrix} \tag{6}$$

Similarly, the local influence of the remaining 17 errors of $f_{g_2}^{(1)}, f_{g_3}^{(1)}, \dots, f_{g_{18}}^{(1)}$ on machining accuracy in three directions can be obtained.

3.3 Fluctuation analysis of geometric error

In this paper, a fitting function based on the Fourier series is proposed to find the internal relationship between geometric error and motion displacement. The fitting function of error g_i is represented by symbol $F_{g_i}(u)$. u is the position of measurement point (i.e., movement axis displacement).

$$F_{g_i}(u) = a_0 + a_1 \cos(wu) + b_1 \sin(wu) + a_2 \cos(2wu) + b_2 \sin(2wu) + a_3 \cos(3wu) + b_3 \sin(3wu) + \dots + a_l \cos(lwu) + b_l \sin(lwu) (l = 1, 2, \dots) \tag{7}$$

Where a_0 is the constant term, $a_1, b_1, a_2, b_2, \dots, a_l, b_l; w$ are the coefficients of the fitting function, and l is the order of the Fourier series.

In addition, the sine series will be used for fitting. The form of the sine series represented by the symbol $S_{g_i}(u)$ is

$$S_{g_i}(u) = p_1 \sin(c_1 u + d_1) + p_2 \sin(c_2 u + d_2) + \dots + p_m \sin(c_m u + d_m) (m = 1, 2, \dots) \tag{8}$$

Where $p_1, c_1, d_1 \dots p_m, c_m, d_m$ are coefficients of the fitting function and m is the order of the sine function.

According to the fitting functions above, this paper uses the fitting function to derive the u . Taking g_1 as an example, formula 9 can be written as follows:

$$f_{g_1}^{(2)} = \frac{1}{n} \left[\sum_{t=1}^n \frac{dF_{g_1}(u)}{d(u)} \Big|_{u=u_t} \right] \tag{9}$$

Where $n (=11)$ is the number of measurement points, $u_t (=50, 130, \dots, 850)$ is the position of measurement points, and $\frac{dF_{g_1}(u)}{d(u)}$ is the fluctuation function of geometric error. The position of the measurement point is brought into the function in turn and then the mean value is calculated. The overall fluctuation of geometric error in the machining stroke can be obtained. Taking the same steps, we can get the fluctuation of the remaining 17 geometric errors, such as $f_{g_2}^{(2)}, f_{g_3}^{(2)}, \dots, f_{g_{18}}^{(2)}$.

3.4 Partial correlation analysis of geometric errors

Pearson product moment correlation is usually used to study the correlation between continuous random variables. In this paper, an improved second-order partial correlation coefficient based on the Pearson product moment is introduced to analyze the correlation between geometric errors. The calculation of the correlation coefficient is shown in Eq. 10–12.

$$R^0_{g_i, g_j} = \text{corrcoef} \left(\begin{matrix} g_i, g_j \\ (i, j = 1, 2, \dots, 18) \end{matrix} \right) \tag{10}$$

$$R^1_{g_i - g_j, g_k} = \frac{R^0_{g_i, g_j} - R^0_{g_i, g_k} \times R^0_{g_j, g_k}}{\sqrt{\left[1 - \left(R^0_{g_i, g_k}\right)^2\right] \left[1 - \left(R^0_{g_j, g_k}\right)^2\right]}} \tag{11}$$

(i, j, k = 1, 2, …18)

$$R^2_{g_i - g_j, g_k - g_h} = \frac{R^1_{g_i - g_j, g_k} - R^1_{g_i - g_j, g_h} \times R^1_{g_k - g_h}}{\sqrt{\left[1 - \left(R^1_{g_i - g_j, g_h}\right)^2\right] \left[1 - \left(R^1_{g_k - g_h, g_i}\right)^2\right]}} \tag{12}$$

(i, j, k, h = 1, 2, …18)

$R^0_{g_i, g_j}$, $R^1_{g_i - g_j, g_k}$, and $R^2_{g_i - g_j, g_k - g_h}$ denote zero-, first-, and second-order partial correlation coefficients, respectively. The result of $R^0_{g_1, g_2}$ is the same as that of $R^0_{g_2, g_1}$, i.e., the result of zero-order correlation can be written as a symmetric matrix with the main diagonal of one. However, in the calculation of the first- and second-order partial correlation, when the errors are the same, the result will be infinite. To ensure that the calculated results can still be written as a matrix form of 18 × 18, so as to clearly show the correlation between the errors, the following provisions are made.

- 1) When two errors are the same (i.e., $i = k$), the calculation result of the first- or second-order partial correlation coefficient is infinite. In this case, refer to the 0-order partial correlation results, and set them to 1. In each case, there are two times of infinity, so it does not affect the calculation results.
- 2) After calculating the first-order partial correlation, 2448 sets of data will be obtained. In order to simplify the calculation, the matrix form of 18 × 18 is still written according to the 0-order calculation results after the average value is calculated for each case. Then, according to the first-order partial correlation formula, the second-order partial correlation coefficient is calculated.

After the second-order partial correlation coefficients of geometric errors in each case are obtained, the mean value is calculated for each case, and the result was still written as the matrix form of 18 × 18. The mean value of each line is calculated again, and the result is taken as the overall correlation between the geometric error and the rest errors. Second-order partial correlation coefficient of single error expressed by $R^2_{g_i}$.

3.5 Establishment of global sensitivity analysis model

Through the above analysis, the global sensitivity model of geometric error is established in the form of sequential multiplication. The symbols $f_X(g_i)$, $f_Y(g_i)$, $f_Z(g_i)$ respectively represent the global sensitivity coefficients of errors to the three machining directions of X, Y, and Z. Equation 13 shows the global sensitivity of the i -th error.

$$f(g_i) = R^2_{g_i} \cdot f^{(1)}_{g_i} \cdot f^{(2)}_{g_i} = \begin{bmatrix} f_X(g_i) & 0 & 0 \\ 0 & f_Y(g_i) & 0 \\ 0 & 0 & f_Z(g_i) \end{bmatrix}$$

$$R^2_{g_i} = \begin{bmatrix} \frac{\partial E_x}{\partial g_i} & 0 & 0 \\ 0 & \frac{\partial E_y}{\partial g_i} & 0 \\ 0 & 0 & \frac{\partial E_z}{\partial g_i} \end{bmatrix} \frac{1}{n} \left[\sum_{t=1}^n \frac{dF_{g_i}(u)}{d(u)} \Big|_{u=u_t} \right] \tag{13}$$

The global sensitivity coefficient of any error g_i to the whole machining space is expressed as $f_{Global}(g_i)$:

$$f_{Global}(g_i) = \sqrt{[f_X(g_i)]^2 + [f_Y(g_i)]^2 + [f_Z(g_i)]^2} \tag{14}$$

4 Case study

4.1 Geometric error measurement and digital characteristics

Under the condition that the testing instrument and the moving axis of the machine tool do not interfere, the

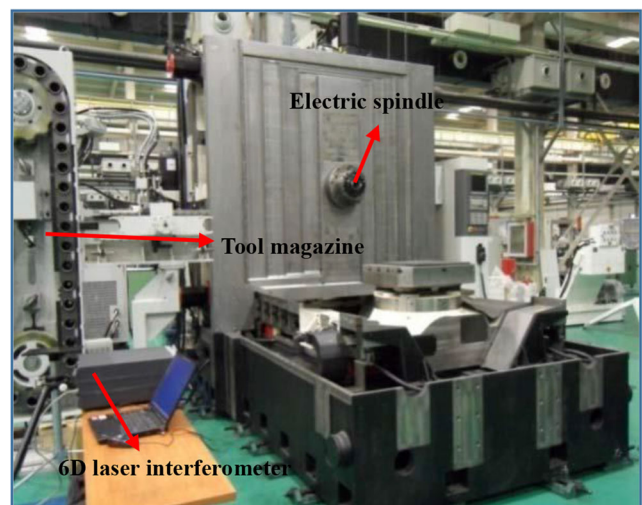


Fig. 4 Error data collection site

Table 4 Geometric error data of X-axis (mm)

u_i	δx_x	δy_x	δz_x	$\varepsilon \alpha_x$	$\varepsilon \beta_x$	$\varepsilon \gamma_x$
50	-8.80e-05	0.00e+00	0.00e+00	1.00e-06	-2.50e-07	-2.00e-06
130	5.25e-04	-1.90e-03	1.85e-03	1.88e-06	-3.25e-06	-2.50e-06
210	1.51e-03	-1.38e-03	3.90e-03	2.88e-06	-6.75e-06	2.88e-06
290	2.68e-03	-8.50e-04	5.43e-03	3.03e-06	-1.11e-05	-2.50e-06
370	3.96e-03	-1.70e-03	7.55e-03	2.50e-06	-1.43e-05	-2.50e-06
450	5.28e-03	-3.60e-03	7.10e-03	1.58e-06	-1.67e-05	-3.75e-06
530	6.93e-03	-4.05e-03	5.70e-03	1.73e-06	-1.91e-05	-5.25e-06
610	8.79e-03	-3.73e-03	4.18e-03	2.40e-06	-1.98e-05	-6.63e-06
690	1.02e-02	-3.00e-03	2.18e-03	3.23e-06	-2.14e-05	-9.25e-06
770	1.16e-02	-2.13e-03	1.95e-03	2.65e-06	-2.33e-05	-1.13e-05
850	1.30e-02	-9.50e-04	0.00e+00	2.57e-06	-2.61e-05	-1.31e-05
Mean value	5.84e-03	-2.12e-03	3.62e-03	2.35e-06	-1.47e-05	-5.08e-06

Table 5 Geometric error data of Y-axis (mm)

u_i	δx_y	δy_y	δz_y	$\varepsilon \alpha_y$	$\varepsilon \beta_y$	$\varepsilon \gamma_y$
50	0.00e+00	-1.25e-03	0.00e+00	-2.13e-06	1.63e-06	1.25e-06
130	-4.50e-04	-6.25e-04	-3.30e-05	-8.75e-07	2.25e-06	2.13e-06
210	6.75e-04	3.00e-04	1.23e-03	-1.88e-06	1.13e-06	2.38e-06
290	2.35e-03	-4.00e-04	6.67e-04	-3.75e-06	-2.13e-06	2.25e-06
370	3.03e-03	2.75e-04	1.23e-03	-3.38e-06	-3.63e-06	1.00e-06
450	1.58e-03	1.13e-03	9.67e-04	-2.63e-06	-2.13e-06	-7.50e-07
530	5.50e-04	3.20e-03	-1.33e-04	-1.38e-06	-2.50e-07	-6.25e-07
610	4.50e-04	5.28e-03	7.00e-04	2.25e-06	-5.00e-07	-1.50e-06
690	-4.50e-04	7.32e-03	3.00e-04	6.50e-06	1.25e-07	-2.63e-06
770	-1.20e-03	8.67e-03	2.33e-04	1.20e-05	6.25e-07	-2.88e-06
850	0.00e+00	9.52e-03	0.00e+00	1.85e-05	-7.50e-07	-2.25e-06
Mean value	5.93e-04	3.04e-03	4.70e-04	2.11e-06	-3.30e-07	-1.48e-07

Table 6 Geometric error data of Z-axis (mm)

u_i	δx_z	δy_z	δz_z	$\varepsilon \alpha_z$	$\varepsilon \beta_z$	$\varepsilon \gamma_z$
50	0.00e+00	0.00e+00	-5.00e-05	-6.25e-06	-3.63e-06	-2.50e-07
130	3.35e-03	1.15e-03	-1.13e-03	-2.75e-05	5.00e-07	1.00e-06
210	5.28e-03	7.50e-05	-6.50e-04	-3.00e-05	2.63e-06	1.88e-06
290	2.80e-03	-1.00e-03	7.50e-04	-1.25e-05	2.63e-06	3.13e-06
370	2.20e-03	-1.23e-03	7.75e-04	-1.88e-05	3.13e-06	3.13e-06
450	4.83e-03	5.00e-04	-1.25e-04	-4.75e-05	6.25e-06	2.75e-06
530	6.33e-03	2.00e-03	-5.50e-04	-6.25e-05	8.38e-06	4.13e-06
610	5.48e-03	1.05e-03	2.83e-03	-3.88e-05	8.25e-06	4.75e-06
690	3.78e-03	-2.50e-04	4.58e-03	-1.75e-05	7.00e-06	5.88e-06
770	2.25e-03	-1.38e-03	7.20e-03	-2.50e-06	7.75e-06	6.38e-06
850	1.30e-03	-8.75e-04	7.13e-03	1.25e-06	9.25e-06	7.75e-06
Mean value	3.42e-03	4.55e-06	1.89e-03	-2.39e-05	4.74e-06	3.68e-06

Table 7 Orientation errors data (mm)

$\varepsilon\gamma_{xy}$	$\varepsilon\beta_{xz}$	$\varepsilon\alpha_{yz}$
9.800e-06	7.000e-06	1.060e-05

same 800 mm stroke is selected on each axis. Take 50 mm as the starting point and set a measuring point at an interval of 80 mm. The moving axis runs twice in both positive and negative directions respectively. Using 6D laser interferometer, each point is measured four times, and the geometric error data at different positions are recorded, as shown in Fig. 4. Statistics and calculation of measured data are shown in Table 4, 5, 6, 7.

4.2 Global sensitivity calculation of geometric errors

According to Section 3.3, some fitting results are shown in Table 8. Figure 5, 6, 7 shows the fitting function of some geometric errors and displacements. All fitting functions of position dependent geometric errors and displacements are shown in Appendix 1 Table 12. Appendix 2 is the second-order partial correlation coefficient of all geometric errors. The direct interaction and potential correlation between errors can be obtained by calculation and analysis.

Among them, R-square represents the quality of a fitting effect. The normal value range is [0,1], the closer it is to 1, it indicates that the variables of the equation have a stronger ability to interpret the function. This model also fits the data well. It can be seen from Appendix 1 Table 12 that most of the R-squares are above 0.98, some are very close to 1. Compared with the low-order Fourier series fitting error-displacement curve based on the least square method of the same guideway in literature [34], the fitting degree of this paper is higher than its 1.7%–8.2%, which can show

the relationship between geometric error and displacement more clearly. Table 9 shows the fitting comparison results. High fitting degree is helpful to analyze the fluctuation of geometric error.

After all the data are brought into the model, Table 10 lists the calculation results of the global sensitivity coefficients of errors. For visual display, the results are shown in histogram 8–9 (Figs. 8 and 9).

From the above figures, the following conclusions can be drawn:

- (1) For the X direction, the global sensitivity coefficients of $\varepsilon\gamma_x, \delta x_x, \varepsilon\beta_x$ are larger. For the Y direction, the global sensitivity coefficients of $\delta y_y, \varepsilon\alpha_y, \delta z_z$ are larger. For the Z direction, the global sensitivity coefficients of $\varepsilon\beta_x, \varepsilon\beta_z, \varepsilon\alpha_y$ are larger. The analysis results show that when the moving parts move along each axis, these three geometric errors and other errors have a great influence on the machining accuracy of each axis through the interaction between them.
- (2) For the whole machining space of machine tools, the global sensitivity coefficients of $\varepsilon\gamma_x, \varepsilon\beta_x, \delta y_y, \delta x_x, \varepsilon\beta_z, \varepsilon\alpha_y$ are relatively large, accounting for 74.6% of the total.

4.3 Application and improvement

From the overall analysis results, the geometric error of X-axis has the greatest impact on the machining accuracy. Therefore, this paper proposes to replace the X-axis with two more accurate guide rails, as shown in Fig. 10. After the improvement, the error is remeasured, and the measurement data is counted and brought into the machine space geometric error model in formula 5. Table 11 shows the accuracy of the machine tool before and after improvement.

Table 8 Fitting functions of partial geometric errors and displacement

Errors	Fitting functions	R-square
X-axis		
δx_x	$F_{g_1}(u) = 0.01234 - 0.007764\cos(0.003396u) - 0.01024\sin(0.003396u) - 0.004848\cos(0.006792u) + 0.001549\sin(0.006792u) + 0.0003975\cos(0.010188u) + 0.001381\sin(0.010188u)$	0.9999
δy_x	$F_{g_2}(u) = 0.002306 + 0.004767\cos(0.004554u) - 0.00667\sin(0.004554u) - 0.002248\cos(0.009108u) - 0.003461\sin(0.009108u) - 0.001832\cos(0.013662u) - 0.0007687\sin(0.013662u)$	0.9946
$\varepsilon\beta_x$	$F_{g_5}(u) = -1.612e-05 + 1.281e-05\cos(0.003927u) + 4.599e-06\sin(0.003927u) + 4.303e-06\cos(0.007854u) - 2.659e-06\sin(0.007854u) - 4.058e-07\cos(0.011781u) - 4.24e-07\sin(0.011781u)$	0.9995
...

Fig. 5 $\delta x_x - u$ fitting curve and residual error

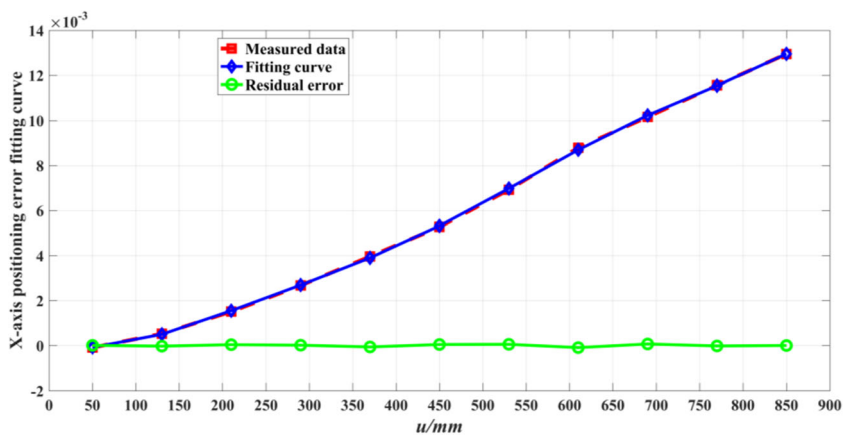


Fig. 6 $\delta y_x - u$ fitting curve and residual error

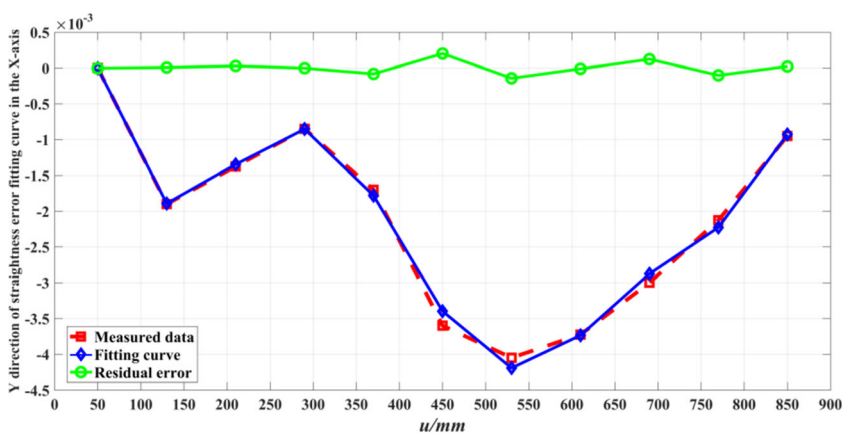


Fig. 7 $\varepsilon \beta_x - u$ fitting curve and residual error

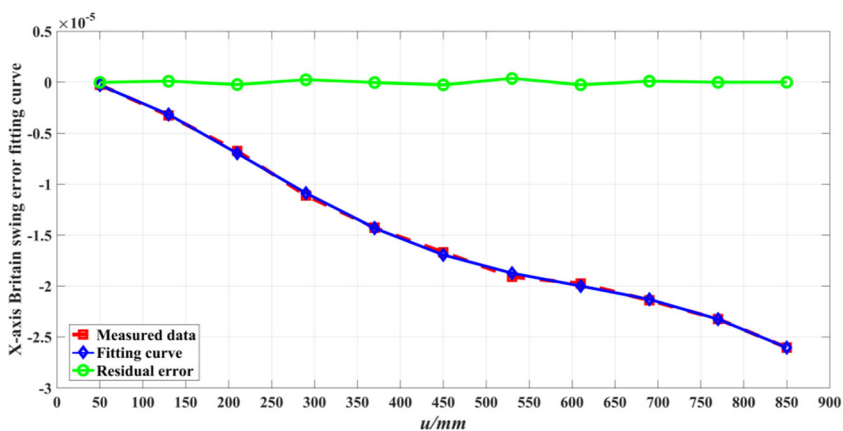


Table 9 Comparison results of R-square

	δx_x	δy_x	δz_x	$\varepsilon \alpha_x$	$\varepsilon \beta_x$	$\varepsilon \gamma_x$
Literature [34]	0.9241	0.9602	0.9245	0.9202	0.9824	0.9613
This paper	0.9999	0.9946	0.9988	0.9926	0.9995	0.9805
Degree of optimization	8.2%	3.5%	8%	7.9%	1.7%	2%

Table 10 The results of global sensitivity coefficients

Number	Errors	$f_X(g_i)$	$f_Y(g_i)$	$f_Z(g_i)$	$f_{Global}(g_i)$
1	δx_x	3.60215e-06	-1.64719e-11	-5.41993e-11	3.60215e-06
2	δy_x	-2.27871e-12	-4.98331e-07	2.22501e-12	4.98331e-07
3	δz_x	-2.62861e-12	-7.80027e-13	-1.747e-07	1.74700e-07
4	$\varepsilon \alpha_x$	7.46418e-12	-2.81626e-07	5.81668e-07	6.46259e-07
5	$\varepsilon \beta_x$	2.83189e-06	3.55494e-13	2.97983e-06	4.11084e-06
6	$\varepsilon \gamma_x$	3.71734e-06	1.89391e-06	-6.43886e-11	4.17199e-06
7	δx_y	3.00344e-07	4.43688e-14	-9.89771e-14	3.00344e-07
8	δy_y	-5.75040e-13	3.89256e-06	-8.22747e-12	3.89256e-06
9	δz_y	-9.30122e-14	-5.96562e-13	-2.82244e-07	2.82244e-07
10	$\varepsilon \alpha_y$	8.79449e-13	-2.30601e-06	1.63494e-06	2.82679e-06
11	$\varepsilon \beta_y$	-3.39646e-07	-8.05578e-13	-3.57395e-07	4.93042e-07
12	$\varepsilon \gamma_y$	1.42438e-07	2.11402e-07	-4.93768e-13	2.54911e-07
13	δx_z	2.99956e-12	-8.34723e-13	1.36057e-07	1.36057e-07
14	δy_z	-2.32242e-07	1.062e-12	5.1201e-12	2.32242e-07
15	δz_z	-8.93720e-12	-1.95441e-06	-1.19904e-11	1.95441e-06
16	$\varepsilon \alpha_z$	1.64095e-06	-3.23157e-07	-3.81595e-11	1.67246e-06
17	$\varepsilon \beta_z$	-5.76688e-11	7.51127e-07	-2.77159e-06	2.87157e-06
18	$\varepsilon \gamma_z$	-5.35722e-07	6.1422e-14	3.89309e-07	6.62238e-07

The experimental results show that this method can effectively identify the geometric errors which have a great influence on the machining accuracy of HMC. The manufacturing and assembly of machine tools should be strictly controlled to fundamentally improve the processing quality of products. At the same time, the validity of the proposed method is proved.

5 Conclusion

The method proposed in this paper has the following features:

- (1) This paper analyzes the overall effect of geometric error on machining accuracy in a certain stroke. By

Fig. 8 Global sensitivity coefficients of geometric errors in X, Y, and Z machining directions

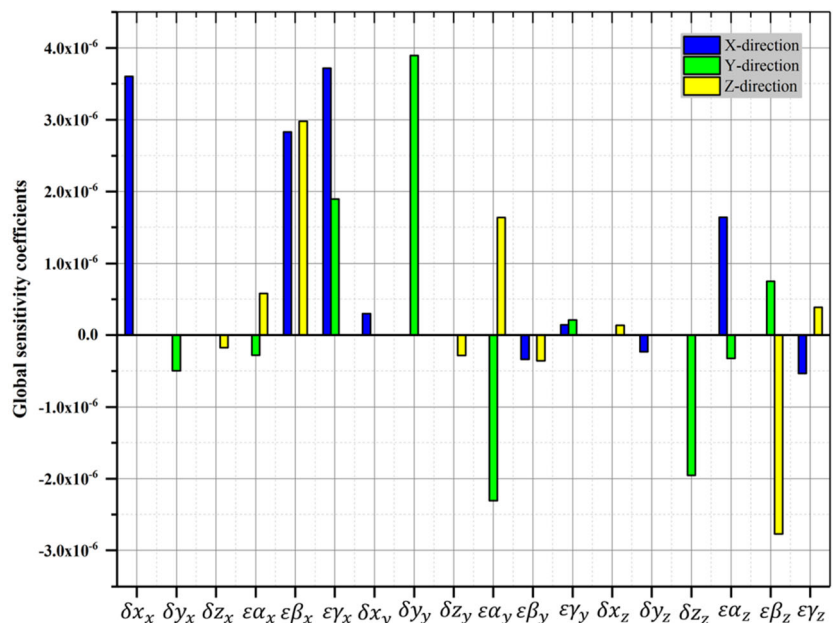


Fig. 9 Global sensitivity of geometric errors in the whole machining space

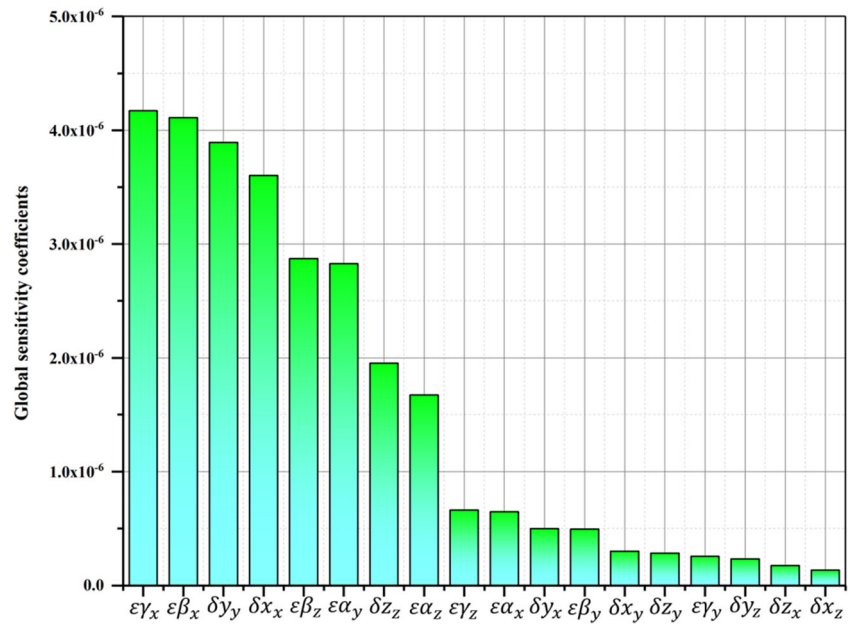
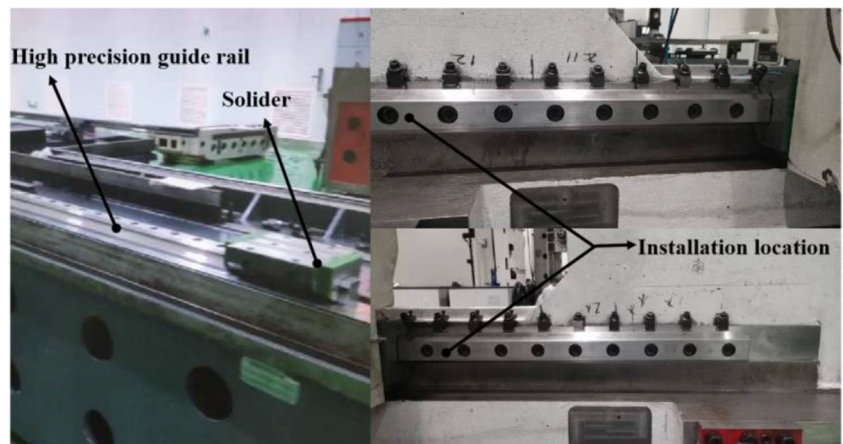


Fig. 10 Replacing high precision guide rail



introducing different displacement points into the fluctuation function, the fluctuation of geometric error at this point can be obtained, and then, the global sensitivity coefficient at this point can be calculated. This method reveals the influence of geometric error on the machining accuracy of machine tool due to the change of movement

position. At the same time, it shows that the sensitivity coefficient changes with the change of displacement.
 (2) In this paper, the Fourier series is used to fit a single geometric error. The results show that the fitting degree is high and the residual error is small. In fact, if the trigonometric function terms in the Fourier series and

Table 11 Accuracy of machine tool before and after improvement

Machining accuracy	Before improvement (mm)	After improvement (mm)
$E_x(G)$	-0.0041	-0.0035
$E_y(G)$	-0.0027	-0.0020
$E_z(G)$	0.0083	0.0059

sine series expand according to Taylor series and ignore the higher-order terms, they are polynomial functions. Therefore, trigonometric functions are more fitting accurate than polynomials. In addition, the dynamic effects of the fluctuation and correlation of geometric errors on machining accuracy are considered in the global sensitivity analysis model proposed in this paper. The analysis results are closer to the actual production process.

- (3) In this paper, only the geometric errors related to the moving axis are studied, but the errors related to the rotating axis (B-axis) have not found good fitting functions. And the research is carried out under the quasi-static condition of machine tool. The dynamic fluctuation of error and thermal error caused by different axial acceleration and dynamic load of machine tool should be further considered.

Data availability The authors declare that all data and material support their published claims and comply with field standards.

Authors' contributions All the authors on this list contributed to this article.

Funding The authors disclosed receipt of the following financial support for the research, authorship, and/or publication of this article: This work was supported by National Science and Technology Major Project (2018ZX04033001–003) and the National Natural Science Foundation of China (51575010).

Compliance with ethical standards

Conflicts of interest/competing interests The authors declared no potential conflicts of interest with respect to the research, authorship and/or publication of this article.

Consent to participate The authors declares that they consent to participate this paper;

Consent to publish The authors declares that they consent to publish this paper;

Code availability Not applicable.

A

Table 12 All fitting functions of position dependent geometric errors and displacements

Errors	Fitting functions	R-square
X-axis		
δx_x	$F_{g_1}(u) = 0.01234 - 0.007764\cos(0.003396u) - 0.01024\sin(0.003396u) - 0.004848\cos(0.006792u) + 0.001549\sin(0.006792u) + 0.0003975\cos(0.010188u) + 0.001381\sin(0.010188u)$	0.9999
δy_x	$F_{g_2}(u) = 0.002306 + 0.004767\cos(0.004554u) - 0.00667\sin(0.004554u) - 0.002248\cos(0.009108u) - 0.003461\sin(0.009108u) - 0.001832\cos(0.013662u) - 0.0007687\sin(0.013662u)$	0.9946
δz_x	$F_{g_3}(u) = 0.003861 - 0.003332\cos(0.007596u) - 0.0001796\sin(0.007596u) + 0.0001561\cos(0.015192u) - 0.0003273\sin(0.015192u) - 0.0001535\cos(0.022788u) - 0.0002358\sin(0.022788u) + 0.0001323\cos(0.030384u) - 0.0004317\sin(0.030384u)$	0.9988
$\varepsilon\alpha_x$	$F_{g_4}(u) = 1.42e-05 + 1.76e-06\cos(0.003927u) - 2.071e-05\sin(0.003927u) + 0.0001561\cos(0.015192u) - 0.0003273\sin(0.015192u) - 0.0001535\cos(0.022788u) - 0.0002358\sin(0.022788u) + 0.0001323\cos(0.030384u) - 0.0004317\sin(0.030384u)$	0.9926
$\varepsilon\beta_x$	$F_{g_5}(u) = -1.612e-05 + 1.281e-05\cos(0.003927u) + 4.599e-06\sin(0.003927u) + 4.303e-06\cos(0.007854u) - 2.659e-06\sin(0.007854u) - 4.058e-07\cos(0.011781u) - 4.24e-07\sin(0.011781u)$	0.9995
$\varepsilon\gamma_x$	$F_{g_6}(u) = 0.07392 - 0.07305\cos(0.001963u) - 0.09616\sin(0.001963u) - 0.0173\cos(0.003926u) + 0.06189\sin(0.003926u) + 0.01898\cos(0.005889u) - 0.007432\sin(0.005889u) - 0.00251\cos(0.007852u) - 0.001562\sin(0.007852u)$	0.9805
Y-axis		
δx_y	$F_{g_7}(u) = 0.001162 + 0.0004632\cos(0.005u) - 0.0002024\sin(0.005u) - 0.001348\cos(0.01u) - 0.00136\sin(0.01u) - 0.0004027\cos(0.014997u) + 1.545e-06\sin(0.014997u) + 0.0005354\cos(0.019996u) + 0.0003185\sin(0.019996u)$	0.9971
δy_y	$S_{g_8}(u) = 0.006983\sin(0.003452u - 0.8668) + 0.003156\sin(0.007368u + 1.315)$	0.9961

Table 12 (continued)

Errors	Fitting functions	R-square
δz_y	$F_{g_9}(u) = 0.0005617 - 0.0004177\cos(0.007847u) + 0.0001527\sin(0.007847u) + 3.794e-07\cos(0.015694u) - 0.0002773\sin(0.015694u) - 0.0001576\cos(0.023541u) - 0.0001097\sin(0.023541u) + 0.0003784\cos(0.031388u) + 0.000159\sin(0.031388u)$	0.9996
$\varepsilon\alpha_y$	$F_{g_{10}}(u) = -7.906e-05 + 1.786e-05\cos(0.002618u) + 0.0001357\sin(0.002618u) + 6.58e-05\cos(0.005236u) - 3.253e-05\sin(0.005236u) - 1.024e-05\cos(0.007854u) - 1.083e-05\sin(0.007854u)$	0.9989
$\varepsilon\beta_y$	$F_{g_{11}}(u) = 2.066e.05 + 1.497e-05\cos(0.003927u) - 3.521e-05\sin(0.003927u) - 1.86e-05\cos(0.007854u) - 1.874e-05\sin(0.007854u) - 1.282e-05\cos(0.011781u) + 7.268e-06\sin(0.011781u) + 2.811e-07\cos(0.015708u) + 5.175e-06\sin(0.015708u)$	0.9962
$\varepsilon\gamma_y$	$F_{g_{12}}(u) = -3.697e-05 - 1.051e-05\cos(0.003927u) + 6.344e-05\sin(0.003927u) + 3826e-05\cos(0.007854u) + 1.645e-05\sin(0.007854u) + 1.027e-05\cos(0.011781u) - 1.595e-05\sin(0.011781u) - 3.937e-06\cos(0.015708u) + 3.381e-06\sin(0.015708u)$	0.9966
Z-axis		
δx_z	$F_{g_{13}}(u) = 0.1964 + 0.01992\cos(0.003476u) - 0.3314\sin(0.003476u) - 0.2072\cos(0.006952u) - 0.02694\sin(0.006952u) - 0.01882\cos(0.010428u) + 0.08538\sin(0.010428u) + 0.018\cos(0.013904u) + 0.008086\sin(0.013904u)$	0.9997
δy_z	$S_{g_{14}}(u) = 0.001435\sin(0.01489u - 0.3582) + 0.0004652\sin(0.00695u - 2.208) + 0.0002184\sin(0.03024u - 1.428)$	0.9951
δz_z	$F_{g_{15}}(u) = 0.00244 + 0.000194\cos(0.005705u) - 0.003774\sin(0.005705u) - 0.001469\cos(0.01141u) - 0.0005427\sin(0.01141u) + 0.0004618\cos(0.017115u) - 0.0004421\sin(0.017115u)$	0.9886
$\varepsilon\alpha_z$	$F_{g_{16}}(u) = -0.003617 - 0.000194\cos(0.003927u) + 0.0005716\sin(0.003927u) + 0.0003601\cos(0.007854u) + 0.0002111\sin(0.007854u) - 0.0001357\cos(0.011751u) - 0.0001378\sin(0.011781u) - 1.683e-05\cos(0.025708u) - 5.997e-05\sin(0.015)$	0.997
$\varepsilon\beta_z$	$F_{g_{17}}(u) = 3.484e-06 - 3.097e-06\cos(0.003927u) + 1.407e-06\sin(0.0003) + 9.772e-08\cos(0.007854u) - 3.246e-07\sin(0.007854u) - 3.604e-06\cos(0.011781u) - 1.217e-06\sin(0.011781u) - 1.845e-06\cos(0.015708u) + 2.527e-06\sin(0.015708u)$	0.9996
$\varepsilon\gamma_z$	$F_{g_{18}}(u) = 9.119e-06 - 2.276e-06\cos(0.003927u) - 9.908e-06\sin(0.003927u) - 5.609e-06\cos(0.007854u) - 4.455e-07\sin(0.007854u) - 9.924e-07\cos(0.011781u) + 1.847e-06\sin(0.011781u)$	0.9916

B

References

1. Yang SH, Kim KH, Park YK, Lee SG (2004) Error analysis and compensation for the volumetric errors of a vertical machining centre using a hemispherical helix ball bar test. Int J Adv Manuf Technol 23(7–8):495–500
2. Cai L, Zhang Z, Cheng Q, Liu Z, Gu P (2015) A geometric accuracy design method of multi-axis nc machine tool for improving machining accuracy reliability. Eksploatacja I Niezawodnos-Maint Reliab 17(1):143–155
3. Yao XP, Hu T, Yin GF, Cheng CH (2020) Thermal error modeling and prediction analysis based on OM algorithm for machine tool's spindle. Int J Adv Manuf Technol 106(7–8):3345–3356
4. Zhang LX, Gong WJ, Zhang K, Wu YH, An D, Shi H, Shi Q (2018) Thermal deformation prediction of high-speed motorized spindle

- based on biogeography optimization algorithm. *Int J Adv Manuf Technol* 97(5–8):3141–3151
5. Yu HZ, Qin SF, Ding GF, Jiang L, Han L (2019) Integration of tool error identification and machining accuracy prediction into machining compensation in flank milling. *Int J Adv Manuf Technol* 102(9–12):3121–3134
 6. Li ZH, Feng WL, Yang JG, Huang YQ (2018) An investigation on modeling and compensation of synthetic geometric errors on large machine tools based on moving least squares method. *Proc Inst Mech Eng Part B-J Eng Manuf* 232(3):412–427
 7. Florussen GHJ, Delbressine FLM, van de Molengraft MJG, Schellekens PHJ (2001) Assessing geometrical errors of multi-axis machines by three-dimensional length measurements. *Measurement* 30(4):241–255
 8. Xu C, Gertner G (2007) Extending a global sensitivity analysis technique to models with correlated parameters. *Comput Stat Data Anal* 51(12):5579–5590
 9. Karkee M, Steward BL (2010) Local and global sensitivity analysis of a tractor and single axle grain cart dynamic system model. *Biosyst Eng* 106(4):352–366
 10. Li Q, Wang W, Jiang Y, Li H, Zhang J, Jiang Z (2018) A sensitivity method to analyze the volumetric error of five-axis machine tool. *Int J Adv Manuf Technol* 98(5–8):1791–1805
 11. Li J, Xie FG, Liu XJ (2016) Geometric error modeling and sensitivity analysis of a five-axis machine tool. *Int J Adv Manuf Technol* 82(9–12):2037–2051
 12. Nojedeh MV, Habibiand M, Arezoo B (2011) Tool path accuracy enhancement through geometrical error compensation. *Int J Mach Tools Manuf* 51(6):471–482
 13. Cheng Q, Zhao HW, Zhang GJ, Gu PH, Cai LG (2014) An analytical approach for crucial geometric errors identification of multi-axis machine tool based on global sensitivity analysis. *Int J Adv Manuf Technol* 75(1–4):107–121
 14. Xia CJ, Wang SL, Ma C, Wang SB, Xiao YL (2020) Crucial geometric error compensation towards gear grinding accuracy enhancement based on simplified actual inverse kinematic model. *Int J Mech Sci* 169:20
 15. Guo SJ, Zhang DS, Xi Y (2016) Global quantitative sensitivity analysis and compensation of geometric errors of CNC machine tool. *Math Probl Eng* 2016:12
 16. Wu HR, Zheng HL, Wang WK, Xiang XP, Rong ML (2020) A method for tracing key geometric errors of vertical machining center based on global sensitivity analysis. *Int J Adv Manuf Technol* 106(9–10):3943–3956
 17. Moon SK, Moon YM, Kota S, Landers RG (2001) Screw theory based metrology for design and error compensation of machine tools. In: *In Proceedings of DETC*, vol 1, pp 697–707
 18. Yang JX, Mayer JRR, Altintas Y (2015) A position independent geometric errors identification and correction method for five-axis serial machines based on screw theory. *Int J Mach Tool Manu* 95:52–66
 19. Guo HC, Yang XJ, Wang SL, Dai ZM (2020) Research on the application of multiplication dimension reduction method in global sensitivity analysis of CNC machine tools. *AIP Adv* 10(1):5
 20. Guo SJ, Jiang GD, Mei XS (2017) Investigation of sensitivity analysis and compensation parameter optimization of geometric error for five-axis machine tool. *Int J Adv Manuf Technol* 93(9–12):3229–3243
 21. Chen BK, Peng CY, Huang J (2019) A new error model and compensation strategy of angle encoder in torsional characteristic measurement system. *Sensors* 19(17):14
 22. Xiang S (2016) Volumetric error measuring and compensation technique for five-axis machine tools. Shanghai Jiao Tong University, Dissertation
 23. Tian W (2014) Investigation into accuracy design and error compensation of high-precision horizontal machining centers. Tianjin University, Dissertation
 24. Fu GQ, Zhang L, Fu JZ, Gao HL, Jin Y (2018) F test-based automatic modeling of single geometric error component for error compensation of five-axis machine tools. *Int J Adv Manuf Technol* 94(9–12):4493–4505
 25. Ekinci TO, Mayer JRR (2007) Relationships between straightness and angular kinematic errors in machines. *Int J Mach Tools Manuf* 47(12–13):1997–2004
 26. Tang H, Duan JA, Zhao QC (2017) A systematic approach on analyzing the relationship between straightness & angular errors and guideway surface in precise linear stage. *Int J Mach Tools Manuf* 120:12–19
 27. Guo SJ, Tang SF, Zhang DS (2019) A recognition methodology for the key geometric errors of a multi-axis machine tool based on accuracy retentivity analysis. *Complexity* 2019:21
 28. Guo S, Mei X, Jiang G, Zhang D, Hui Y (2016) Correlation analysis of geometric error for CNC machine tool. *Nongye Jixie Xuebao/Transac Chin Soc Agric Mach* 47(10):383–389
 29. Cheng Q, Dong LF, Liu ZF, Li JY, Gu PH (2018) A new geometric error budget method of multi-axis machine tool based on improved value analysis. *Proc Mechan Eng Part C-J Mech Eng Sci* 232(22):4064–4083
 30. Chen JX, Lin SW, Zhou XL (2016) A comprehensive error analysis method for the geometric error of multi-axis machine tool. *Int J Mach Tools Manuf* 106:56–66
 31. de la Fuente A, Bing N, Hoeschele I, Mendes P (2004) Discovery of meaningful associations in genomic data using partial correlation coefficients. *Bioinformatics* 20(18):3565–3574
 32. Han L, Zhu J (2008) Using matrix of thresholding partial correlation coefficients to infer regulatory network. *Biosystems* 91(1):158–165
 33. Song YF, Kube CM, Zhang J, Li XB (2020) Higher-order spatial correlation coefficients of ultrasonic backscattering signals using partial cross-correlation analysis. *J Acoust Soc Am* 147(2):757–768
 34. Fan JW, Tao HW, Wu CJ, Pan R, Tang YH, Li ZS (2018) Kinematic errors prediction for multi-axis machine tools' guideways based on tolerance. *Int J Adv Manuf Technol* 98(5–8):1131–1144

Publisher's note Springer Nature remains neutral with regard to jurisdictional claims in published maps and institutional affiliations.